Crank–Nicolson FDTD Method in Media Described by Time-Fractional Constitutive Relations

Damian Trofimowicz*, Tomasz P. Stefański*, Jacek Gulgowski†,
*Faculty of Electronics, Telecommunications and Informatics, Gdansk University of Technology, Gdansk, Poland,
d.trofimowicz@gmail.com, tomasz.stefanski@pg.edu.pl
†Faculty of Mathematics, Physics and Informatics, University of Gdansk, Gdansk, Poland,
jacek.gulgowski@ug.edu.pl

***Abstract*—In this contribution, we present the Crank-Nicolson finite-difference time-domain (CN-FDTD) method, implemented for simulations of wave propagation in media described by time-fractional (TF) constitutive relations. That is, the considered constitutive relations involve fractional-order (FO) derivatives based on the Grünwald-Letnikov definition, allowing for description of hereditary properties and memory effects of media and processes. Therefore, the TF constitutive relations make it possible to include, in a dielectric response, diffusion processes which are modelled mathematically by the diffusion-wave equation.**

We formulate fundamental equations of the proposed CN-FDTD method, and then we execute simulations which confirm its accuracy and applicability. Additionally, we perform numerical tests of stability, which confirm unconditional stability of the method. The proposed method is useful for researchers investigating numerical techniques in media described by FO derivatives.

***Index Terms*—finite-difference time-domain, Crank-Nicolson method, fractional calculus, Grünwald-Letnikov derivative, computational electromagnetics.**

I. Introduction

The finite-difference time-domain (FDTD) method [1] is one of the flagship computational tools, whose accuracy and usefulness are proven in solving real-world electromagnetics problems. It belongs to the class of grid-based differential methods, which discretize time-dependent Maxwell's equations in partial-differential form with the use of central-difference approximations to partial derivatives. Then the obtained equations are solved with the use of an explicit time stepping scheme, i.e., the so-called *leapfrog* integration scheme. Unfortunately, the efficiency of FDTD is limited due to the Courant-Friedrich-Lewy (CFL) stability constraint [2], which limits the maximum stable time-step size applicable in this method. In order to avoid this issue, various implicit integration schemes were proposed, including the Crank-Nicolson (CN) method. Its fundamental application to the FDTD scheme is presented in [3], [4], whilst its application to dispersive materials is formulated in [5]. Afterwards, the analysis of microwave circuits with the use of CN-FDTD is demonstrated in [6].

In this contribution, we demonstrate the application of the CN-FDTD method to analyse wave propagation in media described by time-fractional (TF) constitutive relations. That is, the media are described by fractional-order (FO) derivatives in the time domain allowing for description of hereditary properties and memory effects of media and processes [7], [8], [9]. Therefore, the TF constitutive relations allow for inclusion of diffusion processes, which are modelled mathematically by the diffusion-wave equation, in a dielectric response. This equation interpolates between the diffusion equation and the wave equation, which behave quite differently concerning their response to a localized disturbance.

We start with a short introduction of the mathematical notation used throughout the paper. In Section III, the TF constitutive relations are introduced. The CN-FDTD method for TF constitutive relations is presented in Section IV, whereas numerical results obtained for this method are presented in Sections V. Finally, we draw a conclusion in Section VI. We believe that the proposed CN-FDTD method is useful for researchers interested in numerical techniques applicable to the media described by FO derivatives.

II. Preliminaries

In this research, the fractional derivative of the order $\alpha > 0$ is defined based on the Grünwald-Letnikov definition [10, Sec. 20.1-20.4]

$$D^\alpha f(t) = \lim_{h \to 0^+} \frac{\Delta_h^\alpha f(t)}{h^\alpha} \tag{1}$$

where

$$\Delta_h^\alpha f(t) = \sum_{j=0}^{\infty} P_j(\alpha) f(t - jh) \tag{2}$$

$$P_j(\alpha) = (-1)^j \binom{\alpha}{j}. \tag{3}$$

For a sufficiently small step size h, it may be considered as a good approximation of the FO derivative. The Grünwald-Letnikov derivative coincides, for a very broad class of functions, with the Marchaud definition [10, Sec. 5.4-5.5], usually applied by us in previous investigations of TF electrodynamics [7], [8], [9]. That is, both definitions satisfy the linearity and semigroup conditions; they are also representable in the phasor domain [11], [12]. Using (2), we define the fractional difference which allows for approximation of FO models (FOMs)

$$\Delta^\alpha f_n = \sum_{j=0}^{n} P_j(\alpha) q^{-j} f_n \tag{4}$$

where f_n denotes the discrete-time function (i.e., $f_n = f(nT)$, T is the sampling period), q^{-1} denotes the backward-shift operator, and $n \in \mathbb{N} \cup \{0\}$ is the time index. In this research we assume that time-domain functions are causal (i.e., $f(t) = 0$ for $t < 0$). Therefore we set the upper summation limit in (4) to n. For an integer order of the derivative (1), it reduces to the standard form of a derivative definition [13].

III. Media Described by FOMs

Our aim is to implement the CN-FDTD method with the following constitutive relations:

$$\epsilon_\beta \mathbf{E} = D_t^{1-\beta}\mathbf{D}, \quad 0 < \beta \leq 1 \tag{5}$$

$$\mu_\gamma \mathbf{H} = D_t^{1-\gamma}\mathbf{B}, \quad 0 < \gamma \leq 1. \tag{6}$$

For $\beta = 1$ and $\gamma = 1$, one obtains ordinary constitutive relations with the permittivity $\epsilon = \epsilon_1$ and the permeability $\mu = \mu_1$:

$$\mathbf{D} = \epsilon \mathbf{E} \tag{7}$$

$$\mathbf{B} = \mu \mathbf{H}. \tag{8}$$

Therefore, to some extent, (5)–(6) are extensions of the classical macroscopic models of electromagnetic media. However, in order to avoid inconsistency of the units, one assumes the following SI units for the parameters in (5)–(6): $[\epsilon_\beta] = \frac{F}{s^{1-\beta}m}$, $[\mu_\gamma] = \frac{H}{s^{1-\gamma}m}$. The constitutive relations (5)–(6) allow for describing hereditary properties and memory effects of media and processes [14]. In [15], Westerlund and Ekstam demonstrate, experimentally, that purely empiric Curie's law [16] is satisfied by all the dielectrics and insulators. That is, the excitation of a dielectric material between electrodes of a capacitor with a constant DC voltage U_0 at the time $t = 0$ results in the current

$$i(t) = \frac{U_0}{h_1 t^\beta} \tag{9}$$

where $t > 0$, $\beta \in (0, 1)$ denotes the parameter stemming from energy losses, and h_1 describes geometrical and dielectric parameters of such a capacitor. This formula can be generalized towards FOM of a capacitor

$$i(t) = C_\beta D_t^\beta v(t) \tag{10}$$

where D_t^β denotes the FO derivative in the time domain, $C_\beta = \frac{\Gamma(1-\beta)}{h_1}$, $v(t) = U_0 \mathbb{1}(t)$ and $\mathbb{1}(t)$ denotes the Heaviside-step function. In [17], it is demonstrated that the constitutive relation (5) between $\mathbf{D}$ and $\mathbf{E}$ provides the experimentally observed formula (10) for a capacitor when circuit-theory models are formulated for FO RLC lumped elements. In [14], the need for FO derivatives to mathematically model the real-life systems is postulated. The author claims that all the systems include an infinite memory of earlier events. Therefore, one has to include this record of earlier events when using FO derivatives, in order to model mathematically the behaviour of devices and systems. Based on that, as in (5), the classical relation between $\mathbf{B}$ and $\mathbf{H}$ is generalized towards (6).

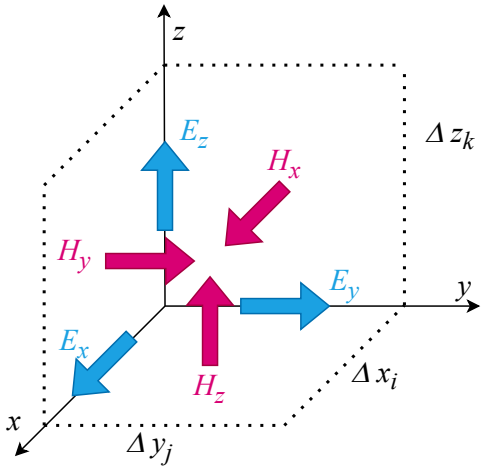

Fig. 1. Yee's grid.

IV. Proposed CN-FDTD Method

A. Spatial Discretization

Using TF derivatives, one can include energy losses in Maxwell's equations. It leads to the following curl equations with FO time derivatives:

$$\nabla \times \mathbf{E} = -\mu_\gamma D_t^\gamma \mathbf{H} - \mathbf{M}_s \tag{11}$$

$$\nabla \times \mathbf{H} = \epsilon_\beta D_t^\beta \mathbf{E} + \mathbf{J}_s \tag{12}$$

where $\mathbf{J}_s$ and $\mathbf{M}_s$ denote, respectively, the electric- and magnetic-current density of sources. These equations can be formulated in the matrix form of state-space equation

$$\begin{bmatrix} D_t^\beta & 0 \\ 0 & D_t^\gamma \end{bmatrix} \begin{bmatrix} \mathbf{E} \\ \mathbf{H} \end{bmatrix} = \begin{bmatrix} 0 & \epsilon_\beta^{-1}[\nabla\times] \\ -\mu_\gamma^{-1}[\nabla\times] & 0 \end{bmatrix} \begin{bmatrix} \mathbf{E} \\ \mathbf{H} \end{bmatrix} + \begin{bmatrix} -\epsilon_\beta^{-1} & 0 \\ 0 & -\mu_\gamma^{-1} \end{bmatrix} \begin{bmatrix} \mathbf{J}_s \\ \mathbf{M}_s \end{bmatrix}. \tag{13}$$

In order to implement CN-FDTD, (13) has to be discretized spatially with the use of Yee's grid [18] (see Fig. 1). For this purpose, the computational domain V (i.e., 3-D cuboid in the Cartesian space) is decomposed into smaller cuboid cells $V_{i,j,k}$ in the following way:

$$V = \{V_{i,j,k} \in \mathbb{R}^3 : [x_i, x_{i+1}] \times [y_j, y_{j+1}] \times [z_k, z_{k+1}]\} \tag{14}$$

where $i = 0, ..., N_x - 1$, $j = 0, ..., N_y - 1$, $k = 0, ..., N_z - 1$. The volume of the cell $V_{i,j,k}$ is equal to $\Delta x_i \Delta y_j \Delta z_k$, where $\Delta x_i = x_{i+1} - x_i$, $\Delta y_j = y_{j+1} - y_j$, $\Delta z_k = z_{k+1} - z_k$. Hence, the total number of cells in the considered domain is equal to $N_x N_y N_z$. Practically, boundary field values are fixed owing to boundary conditions. Hence we assume that the components E_x, E_y, E_z, H_x, H_y, H_z are sampled in N_{ex}, N_{ey}, N_{ez}, N_{hx}, N_{hy}, N_{hz} points, respectively. With such a grid, the

spatial-domain discretization of (13) can be performed. Then one obtains the following state-space equation:

$$\mathbf{D}\mathbf{x} = \mathbf{A}\mathbf{x} + \mathbf{B}\mathbf{u} \tag{15}$$

where

$$\mathbf{D} = \begin{bmatrix} D_t^{\beta} & 0 \\ 0 & D_t^{\gamma} \end{bmatrix}$$

$$\mathbf{A} = \begin{bmatrix} 0 & \epsilon_{\beta}^{-1}[\nabla\times]_D^H \\ -\mu_{\gamma}^{-1}[\nabla\times]_D^E & 0 \end{bmatrix} \tag{16}$$

$$\mathbf{B} = \begin{bmatrix} -\epsilon_{\beta}^{-1}\mathbf{I}_{N_e} & 0 \\ 0 & -\mu_{\gamma}^{-1}\mathbf{I}_{N_h} \end{bmatrix} \tag{17}$$

$$\begin{aligned}\mathbf{x} = [&(E_x)_1, ..., (E_x)_{N_{ex}}, (E_y)_1, ..., (E_y)_{N_{ey}}, \\ &(E_z)_1, ..., (E_z)_{N_{ez}}, (H_x)_1, ..., (H_x)_{N_{hx}}, \\ &(H_y)_1, ..., (H_y)_{N_{hy}}, (H_z)_1, ..., (H_z)_{N_{hz}}]^T\end{aligned}$$

$$\begin{aligned}\mathbf{u} = [&(J_{sx})_1, ..., (J_{sx})_{N_{ex}}, (J_{sy})_1, ..., (J_{sy})_{N_{ey}}, \\ &(J_{sz})_1, ..., (J_{sz})_{N_{ez}}, (M_{sx})_1, ..., (M_{sx})_{N_{hx}}, \\ &(M_{sy})_1, ..., (M_{sy})_{N_{hy}}, (M_{sz})_1, ..., (M_{sz})_{N_{hz}}]^T\end{aligned}$$

where $N_e = N_{ex} + N_{ey} + N_{ez}$, $N_h = N_{hx} + N_{hy} + N_{hz}$, $\mathbf{I}_N$ is the square identity matrix of the size $N \times N$, whilst $[\nabla\times]_D^E$ and $[\nabla\times]_D^H$ are discrete equivalents of the curl operator for the electric- and magnetic-fields, respectively. The matrix operators $[\nabla\times]_D^E$ and $[\nabla\times]_D^H$ of size $N_h \times N_e$ and $N_e \times N_h$, respectively, approximate the curl operator by the difference quotients of the field values in the considered cell $V_{i,j,k}$, and in the neighbouring cells. The spatial discretization has to be sufficiently dense to accurately represent (13) with the use of (15) formulated in the discrete spatial domain.

B. Time Discretization

State-space equations can usually be discretized in the time domain, based on either the forward- or backward-Euler method, as well as with the use of CN method (also called the Tustin method in the control engineering literature) [19]. In this contribution, we focus on CN discretization in the time domain, which is usually computationally expensive but, on the other hand, is accurate and unconditionally stable.

Assuming that the sampling time is T, we denote $\mathbf{x}_n = \mathbf{x}(nT)$ and $\mathbf{u}_{n+\frac{1}{2}} = \frac{1}{2}(\mathbf{u}_{n+1} + \mathbf{u}_n)$. Then we approximate the fractional derivative according to the Grünwald-Letnikov definition (1), assuming the finite time-step size $T > 0$.

1) Case $\beta = \gamma = \nu$: In this case, one obtains

$$\left(\mathbf{I}_N - \frac{T^{\nu}}{2}\mathbf{A}\right)\mathbf{x}_{n+1} = \left(\nu\mathbf{I}_N + \frac{T^{\nu}}{2}\mathbf{A}\right)\mathbf{x}_n + T^{\nu}\mathbf{B}\mathbf{u}_{n+\frac{1}{2}}$$

for $n = 0$ and

$$\begin{aligned}\left(\mathbf{I}_N - \frac{T^{\nu}}{2}\mathbf{A}\right)\mathbf{x}_{n+1} = &\left(\nu\mathbf{I}_N + \frac{T^{\nu}}{2}\mathbf{A}\right)\mathbf{x}_n + T^{\nu}\mathbf{B}\mathbf{u}_{n+\frac{1}{2}} \\ &- \sum_{j=1}^{n} P_{j+1}(\nu)\mathbf{x}_{n-j}\end{aligned} \tag{18}$$

for $n \geq 1$.

2) Case $\beta \neq \gamma$: In this case, one obtains

$$\begin{aligned}\left(\mathbf{I}_N - \frac{1}{2}\mathbf{T}(\beta,\gamma)\mathbf{A}\right)\mathbf{x}_{n+1} = &\left(\mathbf{I}_N + \frac{1}{2}\mathbf{T}(\beta,\gamma)\mathbf{A}\right)\mathbf{x}_n \\ &+ \mathbf{T}(\beta,\gamma)\mathbf{B}\mathbf{u}_{n+\frac{1}{2}}\end{aligned}$$

for $n = 0$ and

$$\begin{aligned}\left(\mathbf{I}_N - \frac{1}{2}\mathbf{T}(\beta,\gamma)\mathbf{A}\right)\mathbf{x}_{n+1} = &\left(\mathbf{I}_N + \frac{1}{2}\mathbf{T}(\beta,\gamma)\mathbf{A}\right)\mathbf{x}_n \\ &+ \mathbf{T}(\beta,\gamma)\mathbf{B}\mathbf{u}_{n+\frac{1}{2}} - \sum_{j=2}^{n+1}\mathbf{P}_j(\beta,\gamma)\mathbf{x}_{n+1-j}\end{aligned} \tag{19}$$

for $n \geq 1$, where

$$\mathbf{P}_j(\beta,\gamma) = \begin{bmatrix} P_j(\beta)\mathbf{I}_{N_e} & 0 \\ 0 & P_j(\gamma)\mathbf{I}_{N_h} \end{bmatrix}$$

$$\mathbf{T}(\beta,\gamma) = \begin{bmatrix} T^{\beta}\mathbf{I}_{N_e} & 0 \\ 0 & T^{\gamma}\mathbf{I}_{N_h} \end{bmatrix}.$$

Usually, the matrices on the left-hand side of the above equations are sparse, hence it is not recommended to invert them to obtain the form resembling standard discrete-time state-space equations, known from control engineering [20]. Otherwise, the application of inverse matrix in the iterative solving procedure would increase the memory consumption and computational overhead of the method.

C. Stability

For electromagnetic systems employing constitutive relations (7)–(8), the CN method is unconditionally stable [4]. In our research, stable simulations with constitutive relations (7)–(8) are modified with FO derivatives. The formal proof that CN discretization is also unconditionally stable for the case with FO derivatives is presented in [21].

V. Simulation Results

The proposed CN-FDTD method is implemented in a code for simulations of one-way propagation of a non-monochromatic plane wave (E_x and H_y components). It allows us to easily refer to the results already presented in the literature [7], in order to prove the correctness of the method. In this simulation scenario, impinging of the plane wave on the half-space described by the TF constitutive relations is considered. Then the wave is transferred into the medium and propagates towards the $+z$ direction. Therefore, the signalling problem is simulated where the electric field at the domain boundary excites the wave. The waveforms at the distance L are computed using both the proposed and the reference methods [7]. We set the order of derivatives $\beta = \gamma = \nu$ at the level slightly below the unit, i.e., only small perturbations of time-derivative orders in Maxwell's equations (11)–(12) are considered. In our research we focus on small perturbations of the parameter ν, in order to obtain characteristics known from wave propagation rather than from diffusion. Let us consider the excitation, which is the Gaussian-modulated sinusoidal pulse as in [7]. The central frequency is set at $f_c = 590$ THz

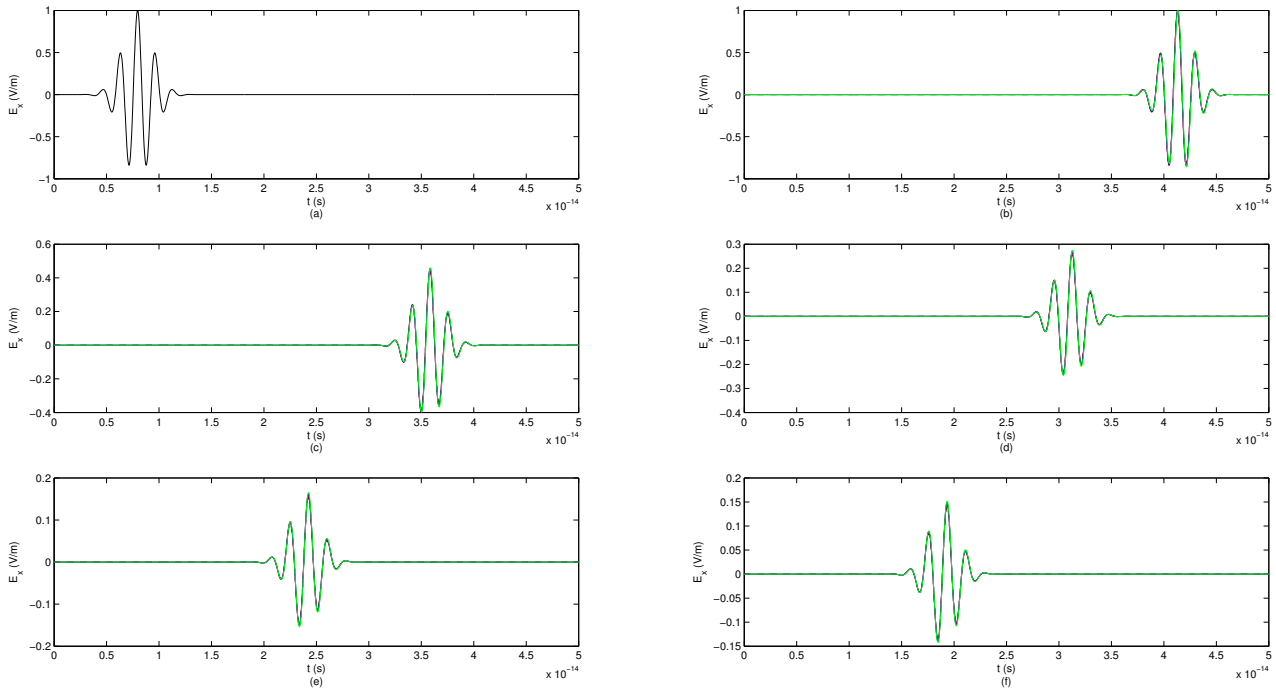

Fig. 2. Propagation of Gaussian-modulated sinusoidal pulse in medium described by TF constitutive relations. Signal measured at distance L = 10 μm. (a) Excitation signal. (b) ν = 1 (vacuum). (c) ν = 0.995. (d) ν = 0.99. (e) ν = 0.98. (f) ν = 0.97. Results are presented for developed CN-FDTD method (— *CFL* = 1, — *CFL* = 3, — *CFL* = 5) and reference method (- -). All lines overlap.

(the wavelength $\lambda_c = 508$ nm in a vacuum) and the spectrum covers the visible band, i.e., 430–750 THz (399–697 nm). Our aim is to increase the time-step size above the standard FDTD stability limit $\Delta t_{FDTD} = \Delta z/c$ (i.e., $\Delta t = \Delta t_{FDTD} CFL$ in our simulations) and reproduce the reference results with the use of CN-FDTD.

The simulation results are shown in Fig. 2, where the waveforms measured at the distance $L = 10$ μm from the source, for varying values of the parameter ν, are demonstrated. The excitation signal is presented in Fig. 2(a), whilst the result for the reference case of a vacuum ($\nu = 1$) is presented in Fig. 2(b). In Figs. 2(c)–(f), values of the parameter ν decrease. Due to a small distance of signal propagation, the pulse-like waveforms are obtained with highly attenuated amplitudes. As one can note, the results obtained with the use of the proposed and reference methods overlap perfectly. Therefore, in Table I, we provide the values of the relative error (in dB) for CN-FDTD with reference to the frequency-domain method. The relative error is, on average, around -36 dB for $CFL = 1$, then it is around -32 dB for $CFL = 3$, and approaches -23 dB for $CFL = 5$. Hence, the relative error increases simultaneously with the CFL factor. However, an increase of the CFL factor allows for speeding up the computations *CFL* times.

In the simulations presented above, the time-step size is greater than the CFL stability limit for standard FDTD. Let us investigate the stability of these CN-FDTD simulations, using the numerical method [22], [23] based on the global

TABLE I
RELATIVE ERROR OF CN-FDTD WITH TF CONSTITUTIVE RELATIONS

ν	*CFL* 1	3	5
1	-34.5	-35.9	-21.3
0.995	-35.3	-34	-22.9
0.99	-35.7	-31.4	-23.4
0.98	-36.3	-29.3	-23.5
0.97	-37.2	-29	-23.9

complex roots and poles finding (GRPF) algorithm [24]. This stability test can be applied if it is possible to formulate the characteristic equation in the form for which the existence of a root inside the unit circle on the complex plane implicates instability. Hence we transfer (19) into the z-domain, assuming that $n \to +\infty$, and subtracting $z = 1/w$. Then one obtains the following characteristic equation for CN-FDTD with the TF constitutive relations (5)–(6):

$$f(w) = \det\left[(1-w)^{\nu}\mathbf{I}_N - \frac{1}{2}T^{\nu}(1+w)\mathbf{A}\right] = 0. \qquad (20)$$

Then, we execute the GRPF algorithm and search for roots of the characteristic equation (20) inside the unit circle at the complex plane. The GRPF algorithm operates on four complex-plane quadrants ($\{Q_1 : 0 \le \arg[f(w)] < \pi/2\}$, $\{Q_2 : \pi/2 \le \arg[f(w)] < \pi\}$, $\{Q_3 : \pi \le \arg[f(w)] < 3\pi/2\}$, $\{Q_4 : 3\pi/2 \le \arg[f(w)] < 2\pi\}$). Roots of the characteristic equation $f(w) = 0$ can be found based on a plane/unit

circle triangulation, and Cauchy's argument principle. If there is a change of phase around a point inside the unit circle, which is equal to $2q\pi$ in the counterclockwise direction, then this point is a root of order q, and the CN-FDTD method is unstable (refer to [24]).

We execute stability tests for CN-FDTD with the parameters *CFL* and ν as for simulation results in Fig. 2. However, we reduce the size of the domain to 64 points in order to finish the tests within a reasonable time. In all the considered cases, we do not obtain roots of the characteristic equation (20) for $|w| < 1$. Although the algorithm detects roots for $|w| = 1$, these are single-order roots, which do not implicate an *explosion* of CN-FDTD solution. A graph of exemplary stability-test results is presented in Fig. 3, where the complex w-plane with phase quadrants of the function $f(w)$ (given by the characteristic equation (20) with $CFL = 5$ and $\nu = 0.97$) is shown. There are 127 complex roots detected around the unit circle by the GRPF algorithm. One of them $w = 1 + 0i$ is located on the unit circle, whereas the remaining ones are outside. These roots are visible as changes of phase between quadrants $Q_1 \to Q_2 \to Q_3 \to Q_4$ in the counterclockwise direction on the complex w-plane (i.e., the colours ■ → ■ → ■ → ■ change in the counterclockwise direction around a considered point). It means that CN-FDTD with the TF constitutive relations (5)–(6) is stable.

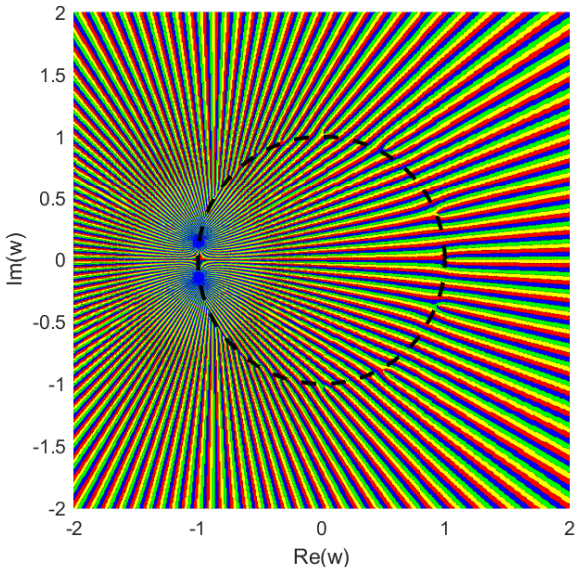

Fig. 3. Quadrants of phase (■ Q_1, ■ Q_2, ■ Q_3, ■ Q_4) for $f(w)$ function when $CFL = 5$ and $\nu = 0.97$. Unit circle is denoted by - -.

VI. Conclusion

We apply the unconditionally-stable CN-FDTD method for simulations of electromagnetic-wave propagation in media described by TF constitutive relations. It is demonstrated that this computational method provides the same results as the frequency-domain reference method already presented in the literature. However, CN-FDTD is extendible towards multidimensional simulations and varying material parameters in the computational domain as a typical finite-difference scheme.

References

[1] A. Taflove and S. C. Hagness, *Computational electrodynamics: the finite-difference time-domain method*, 3rd ed. Norwood: Artech House, 2005.

[2] J. Crank and P. Nicolson, "A practical method for numerical evaluation of solutions of partial differential equations of the heat-conduction type," *Math. Proc. Camb. Philos. Soc.*, vol. 43, no. 1, pp. 50–67, 1947.

[3] G. Sun and C. Trueman, "Unconditionally-stable FDTD method based on Crank-Nicolson scheme for solving three-dimensional Maxwell equations," *Electron. Lett.*, vol. 40, no. 10, pp. 589–590(1), 2004.

[4] Y. Yang, R. Chen, and E. Yung, "The unconditionally stable Crank Nicolson FDTD method for three-dimensional Maxwell's equations," *Microw. Opt. Technol. Lett.*, vol. 48, no. 8, pp. 1619–1622, 2006.

[5] H. Rouf, F. Costen, and S. Garcia, "3D Crank-Nicolson finite difference time domain method for dispersive media," *Electron. Lett.*, vol. 45, no. 19, pp. 961–962(1), 2009.

[6] Y. Yang, R. Chen, D. Wang, and E. Yung, "Unconditionally stable Crank-Nicolson finite-different time-domain method for simulation of three-dimensional microwave circuits," *IET Microw. Antennas Propag.*, vol. 1, no. 4, pp. 937–942(5), 2007.

[7] T. P. Stefański and J. Gulgowski, "Signal propagation in electromagnetic media described by fractional-order models," *Commun. Nonlinear Sci. Numer. Simul.*, vol. 82, p. 105029, 2020.

[8] ——, "Formulation of time-fractional electrodynamics based on Riemann-Silberstein vector," *Entropy*, vol. 23, no. 8, p. 987, 2021.

[9] ——, "Fundamental properties of solutions to fractional-order Maxwell's equations," *J. Electromagn. Waves Appl.*, vol. 34, no. 15, pp. 1955–1976, 2020.

[10] S. G. Samko, A. A. Kilbas, and O. I. Marichev, *Fractional Integrals and Derivatives: Theory and Applications*. Gordon and Breach, New York, 1993.

[11] J. Gulgowski and T. P. Stefański, "On applications of fractional derivatives in electromagnetic theory," in *2020 23rd International Conference on Microwave, Radar and Wireless Communications (MIKON)*, 2020, pp. 1–4.

[12] J. Gulgowski, T. P. Stefański, and D. Trofimowicz, "On applications of elements modelled by fractional derivatives in circuit theory," *Energies*, vol. 13, no. 21, 2020.

[13] E. W. Weisstein, "Derivative," *From MathWorld–A Wolfram Web Resource*, 2023. [Online]. Available: https://mathworld.wolfram.com/Derivative.html

[14] S. Westerlund, "Dead matter has memory!" *Phys. Scr.*, vol. 43, no. 2, pp. 174–179, 1991.

[15] S. Westerlund and L. Ekstam, "Capacitor theory," *IEEE Trans. Dielectr. Electr. Insul.*, vol. 1, no. 5, pp. 826–839, 1994.

[16] M. J. Curie, "Recherches sur la conductibilit des corps cristallises," *Ann. Chim. Phys.*, vol. 18, pp. 203–269, 1889.

[17] T. P. Stefański and J. Gulgowski, "Electromagnetic-based derivation of fractional-order circuit theory," *Commun. Nonlinear Sci. Numer. Simul.*, vol. 79, p. 104897, 2019.

[18] K. Yee, "Numerical solution of initial boundary value problems involving Maxwell's equations in isotropic media," *IEEE Trans. Antennas Propag.*, vol. 14, no. 3, pp. 302–307, 1966.

[19] E. W. Weisstein, "Finite difference," *From MathWorld–A Wolfram Web Resource*, 2023. [Online]. Available: https://mathworld.wolfram.com/FiniteDifference.html

[20] R. J. Vaccaro, *Digital Control*, 1st ed. McGraw-Hill Higher Education, 1995.

[21] U. Ali, F. A. Abdullah, and A. I. Ismail, "Crank-Nicolson finite difference method for two-dimensional fractional sub-diffusion equation," *J. of Interpolation and Approximation in Scientific Computing*, no. 2, pp. 18–29, 2017.

[22] Ł. Grzymkowski, D. Trofimowicz, and T. P. Stefański, "Stability analysis of interconnected discrete-time fractional-order lti state-space systems," *Int. J. Appl. Math. Comput. Sci.*, vol. 30, no. 4, pp. 649–658, 2020.

[23] D. Trofimowicz and T. P. Stefański, "Testing stability of digital filters using optimization methods with phase analysis," *Energies*, vol. 14, no. 5, p. 1488, 2021.

[24] P. Kowalczyk, "Global complex roots and poles finding algorithm based on phase analysis for propagation and radiation problems," *IEEE Trans. Antennas Propag.*, vol. 66, no. 12, pp. 7198–7205, 2018.